Helium Ion Microscopy: A New Tool for Imaging Novel Mesoporous Silica and Organosilica Materials

Supporting Information

S1. General Information

All solvents and reagents including 1,4-bis(triethoxysilyl)benzene (**BTESB**, Gelest) were purchased and used without further purification. Solid-state NMR spectra were collected on a 400 MHz Varian Unity Inova equipped with a Varian/Chemagnetics 4mm T3 MAS probe. ^{13}C CP/MAS experiments (100 MHz, 7000 scans) used glycine as a reference. Samples were spun at a rate of 5 kHz. A contact time of 1.5 ms and recycle delay of 2s was applied. UV-visible/near-IR spectroscopy was conducted on a Cary 5000 UV-Vis/NIR spectrophotometer and CD experiments were performed using a JASCO J-815 spectropolarimeter. Spectra were collected by mounting free-standing films so that the surfaces of the films were perpendicular to the beam path. It is important to note that due to the large CD signal generated by these materials, small pieces of film were used to avoid saturating the detector. Additionally, samples containing larger precursor to silica ratios have more red shifted peaks (above 1100 nm) and could not be detected due to limitation of the CD detector. N_2 adsorption/desorption studies were performed using a Micromeritics ASAP 2000 at 77 K. All samples were degassed under vacuum at 130 °C immediately prior to analysis. BJH pore size distributions were all calculated from the adsorption branch of the isotherm. Thermogravimetric analysis (TGA) was performed on a PerkinElmer Pyris 6 thermogravimetric analyzer and sample was run under air. Elemental analysis was carried out by UBC Microanalytical Services. IR spectra were obtained with a Nicolet 6700 FT-IR equipped with a Smart Orbit diamond ATR.

SEM images were collected on a Hitachi S4700 electron microscope. The sample was prepared by breaking the film into small pieces and attaching the pieces to aluminum stubs using double-sided adhesive tape. The sample was sputter-coated with 5 nm of gold. Helium ion microscopy was performed on a Zeiss Orion Plus Helium Microscope. Dry samples were carefully broken to expose the cross section and then were mounted on a stub so that the cross section is facing up. The advantage of this orientation is that the He ion beam can raster the cross section without needing to tilt the stage. Because the He ion microscope is outfitted with a low energy electron flood gun, which is used to neutralize the ion charging during imaging, non-conductive samples like silica can be imaged easily without sputter-coating. Images were taken at an accelerating voltage of 30-35 kV and at a probe current of 0.1-0.8 pA..

S2. Experimental

Nanocrystalline cellulose (NCC), **CNMS** and **Et-CNMO** were prepared according the literature procedure.[1,2] The NCC suspension was diluted with deionized water to the desired concentration (3.5 wt. %).

Synthesis of Bz-Composite films. The NCC/organosilica films **Bz-Comp,** were prepared using the following general procedure: Ethanol was added to the 3.5 wt. % aqueous NCC suspension up to a concentration of 50% v/v. After 10 min sonication, the organosilica precursor was added dropwise to the NCC suspension (ratios of 2.5-5.0 mmol precursor per gram of NCC were used for **Bz-Comp**) and stirred at room temperature until they appeared homogeneous. The NCC / organosilica precursor mixtures were then transferred to polystyrene Petri dishes (10 mL / 60 mm dish) and left to dry under ambient conditions. The resulting films usually appear iridescent, though in some cases the reflectance was shifted into the near-IR.

Synthesis of chiral nematic mesoporous organosilica: Bz-CNMO and Et-CNMO-HCl. NCC/organosilica composite films were treated in 12 M HCl (~500 mg film / 500 mL 12 M HCl) and heated to 85-95 °C overnight without stirring to avoid breaking the films. After filtration, ~100 mg of films were placed in 30% hydrogen peroxide solution with 15 mg of silver nitrate and heated to 70-90 °C until the films appeared colorless (typically 2 h). The films were then filtered and heated to 70 °C in distilled water overnight before final filtration and air-drying.

We made a range of samples using this general procedure; the following describes the synthesis of **Bz-CNMO** with a ratio of 3.2 mmol **BTESB** per gram of NCC. **BTESB** (1.0 mL, 2.6 mmol) was added dropwise to 24 mL of freshly sonicated 3.5 wt.% aqueous NCC and 24 mL of ethanol. The mixture was stirred for 2 h at room temperature then distributed into five polystyrene Petri dishes (10 mL / 60 mm dish) to evaporate overnight. Composite films were obtained (667 mg) with a reflectance peak at 1530 nm. Composite films were placed in 12 M HCl (~500 mL) and heated to 90 ^{o}C for 24 h. The films were filtered, washed with water and placed in a solution of 30% hydrogen peroxide (75 mL) and silver nitrate (0.041 g) at 90 ^{o}C for 4 h. The films were then filtered, placed in water and heated to 70 ^{o}C overnight. The films were filtered and allowed to air-dry. Free-standing iridescent films (126 mg) with a reflection peak at 790 nm and a CD signal at 730 nm were obtained (note that the discrepancy likely comes from the measurement of different regions of the film and possibly slightly different orientations). Elemental analysis determined: %C 28.51, %H 3.45, which is close to the value calculated for $(C_6H_4Si_2O_3)(H_2O)_4$ (28.56% C, 4.79% H). TGA showed 30 wt % loss of the films indicating decomposition of the phenylene bridge by 700 ^{o}C. In the FT-IR, peaks are observed at 1020 cm^{-1} and 800 cm^{-1} (Si-O stretch), 1155 cm^{-1} and a feature at 2890 cm^{-1} (C-C and C-H stretching, respectively) and a broad peak centered at 3300 cm^{-1} corresponding to uncondensed SiO-H bonds. PXRD displayed broad peaks at 11° and 22° 2θ. N_2 adsorption isotherms indicated a surface area of 740 m^2/g with a specific pore volume of 0.69 cm^3/g and a BJH pore diameter of 5 nm.

S3. Additional characterization of Bz-CNMO, Et-CNMO and Et-CNMO-HCl

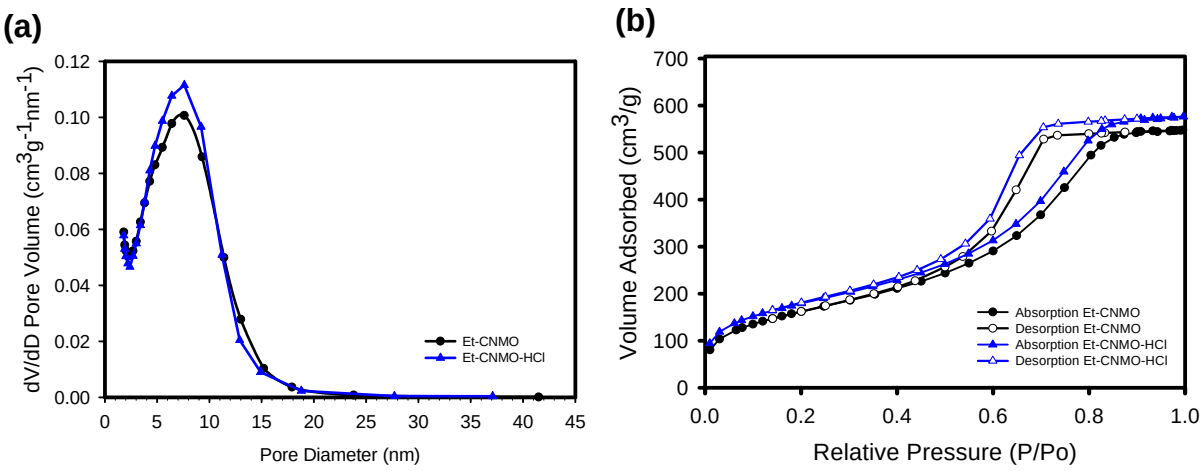

Figure S1. N_2 adsorption data for ethylene-bridged organosilica samples with different acid hydrolysis procedures. NCC was removed with 6M sulfuric acid and 12M HCl for **Et-CNMO** and **Et-CNMO-HCl**, respectively. (a) BJH pore size distribution of **Et-CNMO** (black) and **Et-CNMO-HCl** (blue). (b) N_2 adsorption/desorption isotherm of **Et-CNMO** (black) and **Et-CNMO-HCl** (blue).

Table S1. N_2 adsorption data for ethylene-bridged organosilica films

Sample	Surface Area - BET (m^2/g)	Pore Volume (cm^3/g)	BJH Pore Diameter (nm)
Et-CNMO	594	0.87	7.5
Et-CNMO-HCl	651	0.89	7.5

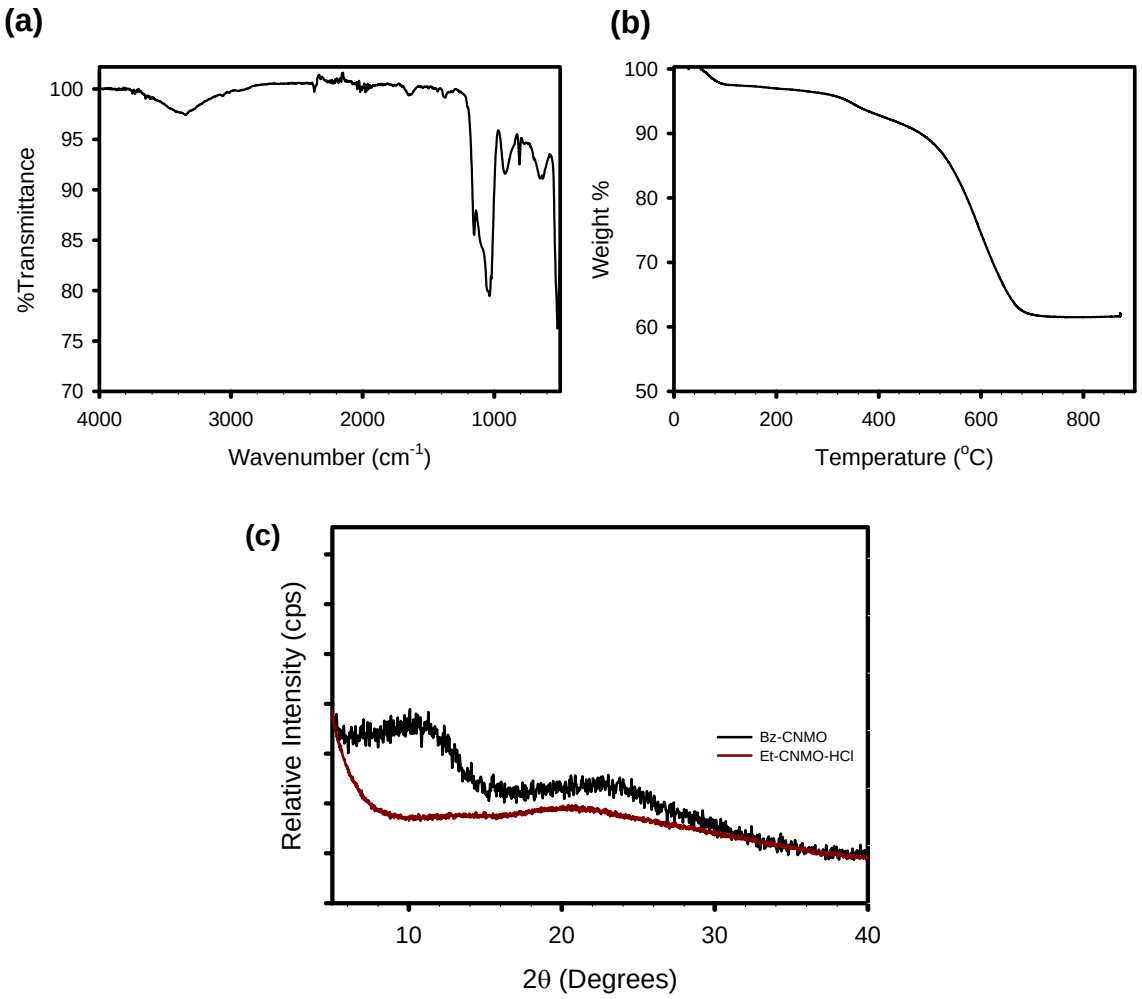

Figure S2. IR spectrum, TGA and PXRD pattern of a typical **Bz-CNMO** sample (a) IR spectrum displays characteristic resonances of phenylene-bridged moiety (C-H, C-C stretching modes) and silica; (b) TGA shows that the phenylene-bridged organosilica is stable up to 300 °C, after which decomposition of 30-35 wt. % occurs. (c) PXRD of **Bz-CNMO** (top) displays two broad peaks located at 11° and 22°. The peaks due to crystalline cellulose are absent. A PXRD pattern of **Et-CNMO-HCl** (bottom) is shown for comparison.

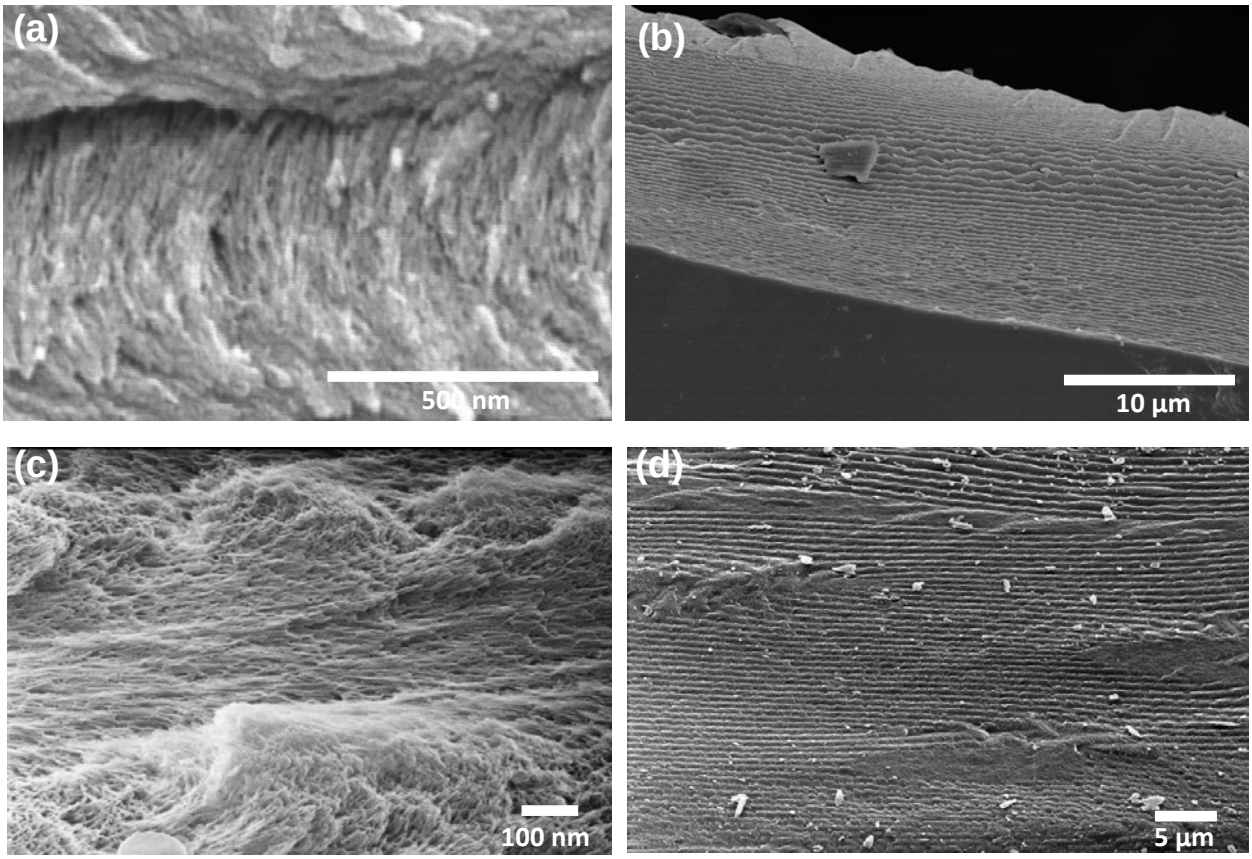

Figure S3. SEM images and HIM images of benzene organosilica samples. (a) High magnification SEM image of **Bz-CNMO** (scale bar = 500nm). (b) SEM of edge of **Bz-CNMO** film at higher magnification (scale bar = 1 µm). (c,d) HIM image of **Bz-CNMO**.

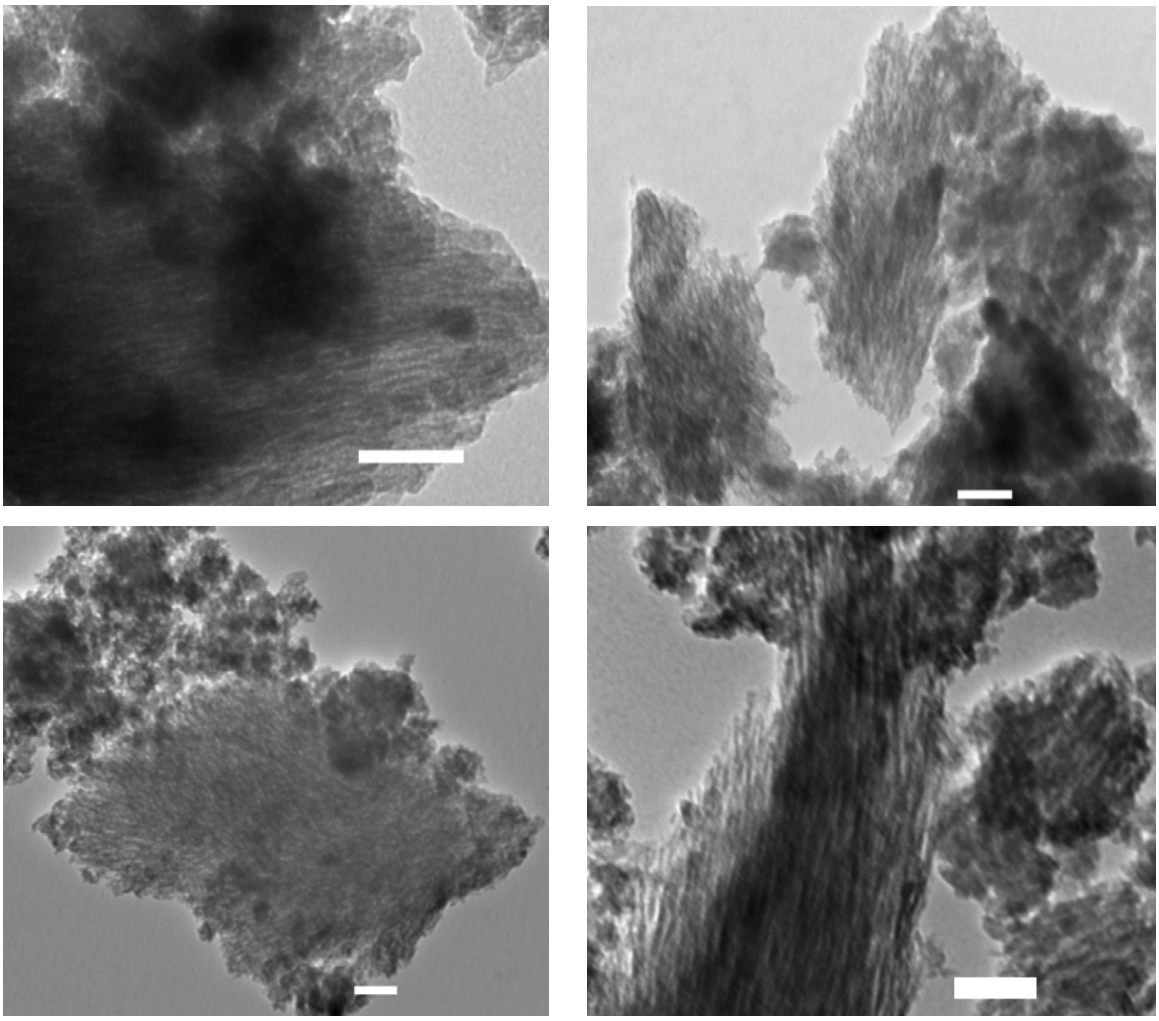

Figure S4. TEM images of four different samples of **Bz-CNMO** that show mesopority and elements of the twisting present in the structures. The scale bar is 100 nm in each image.

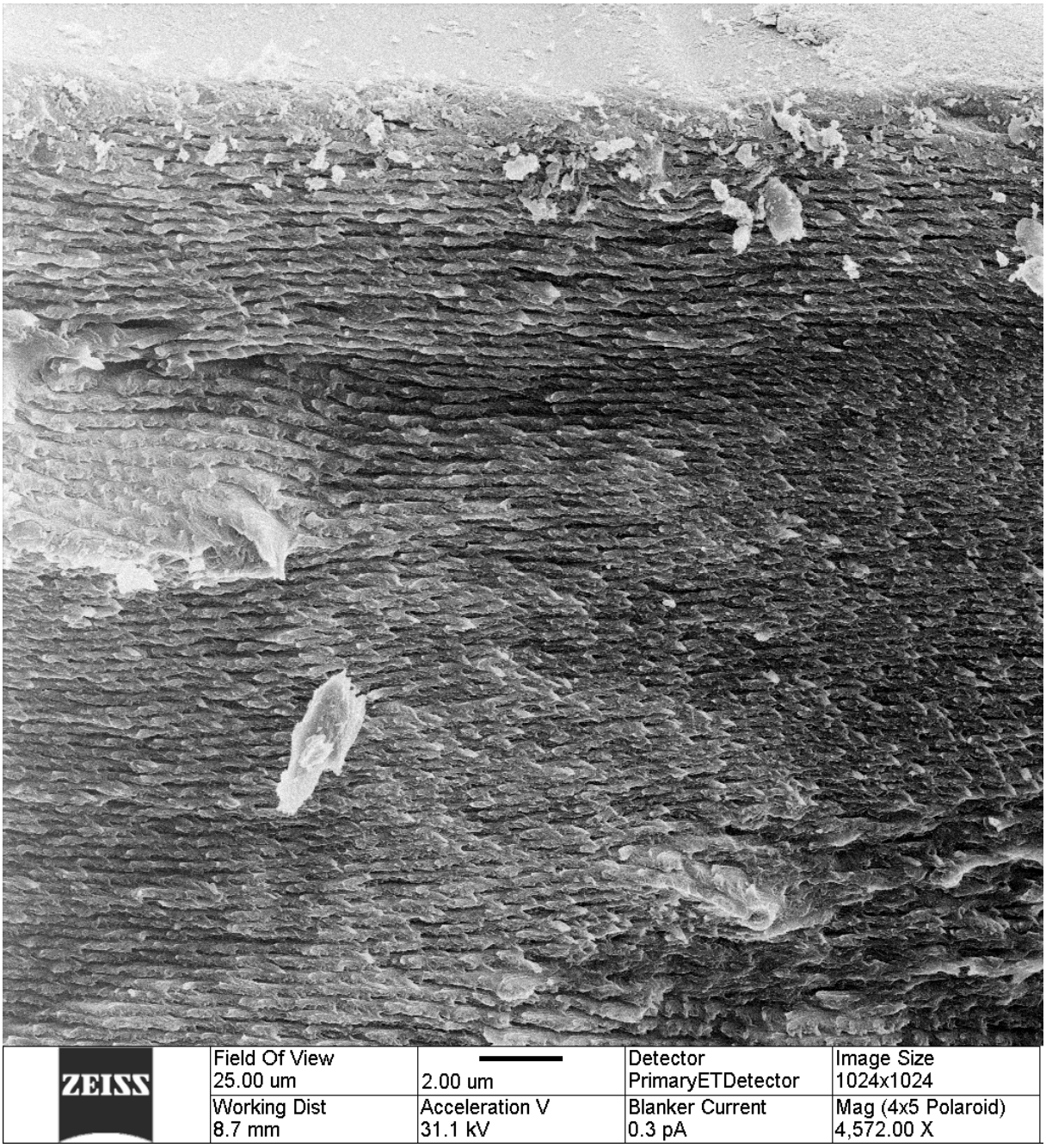

Figure S5. Expanded Figure 2a.

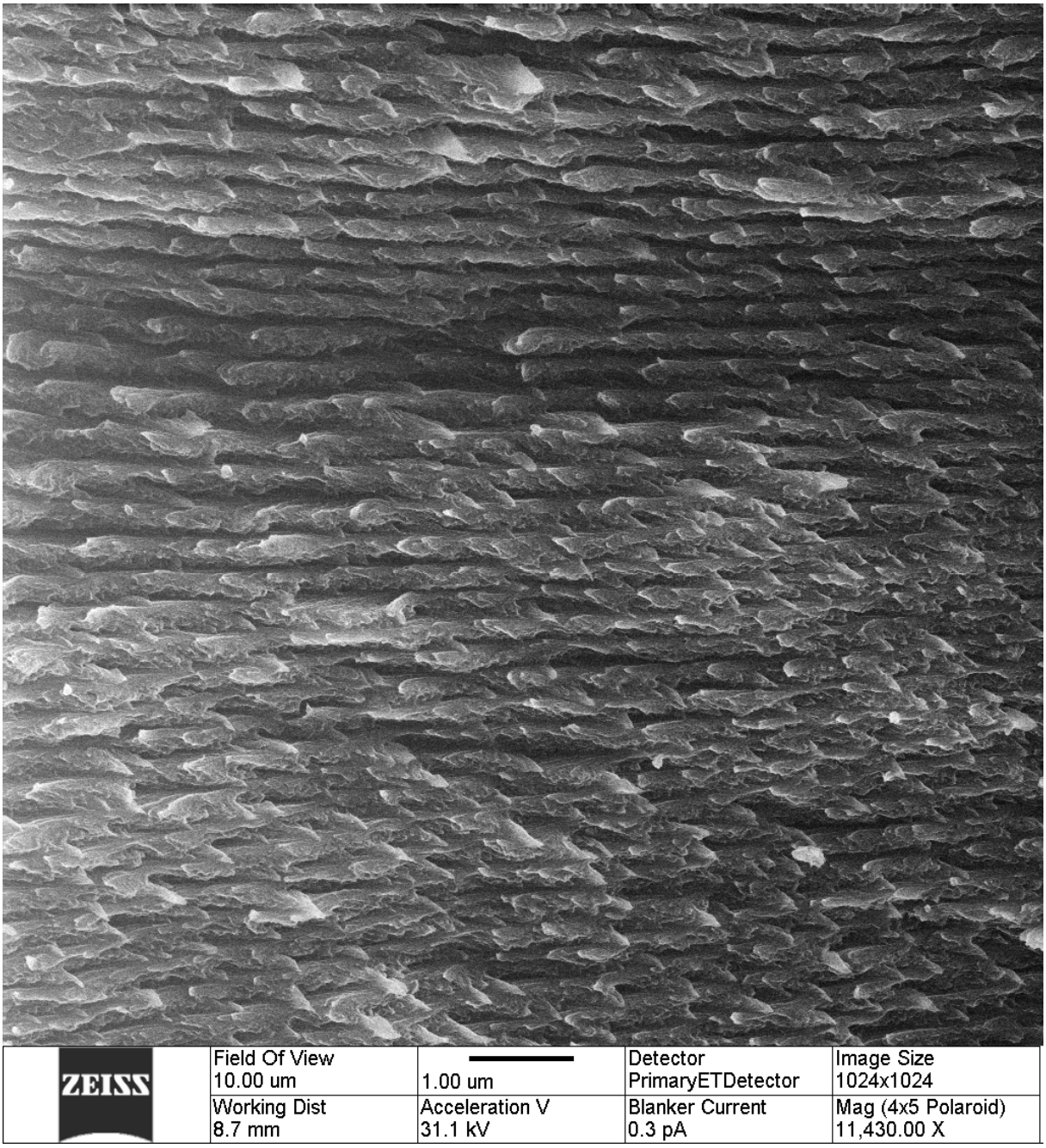

Figure S6. Expanded Figure 2b.

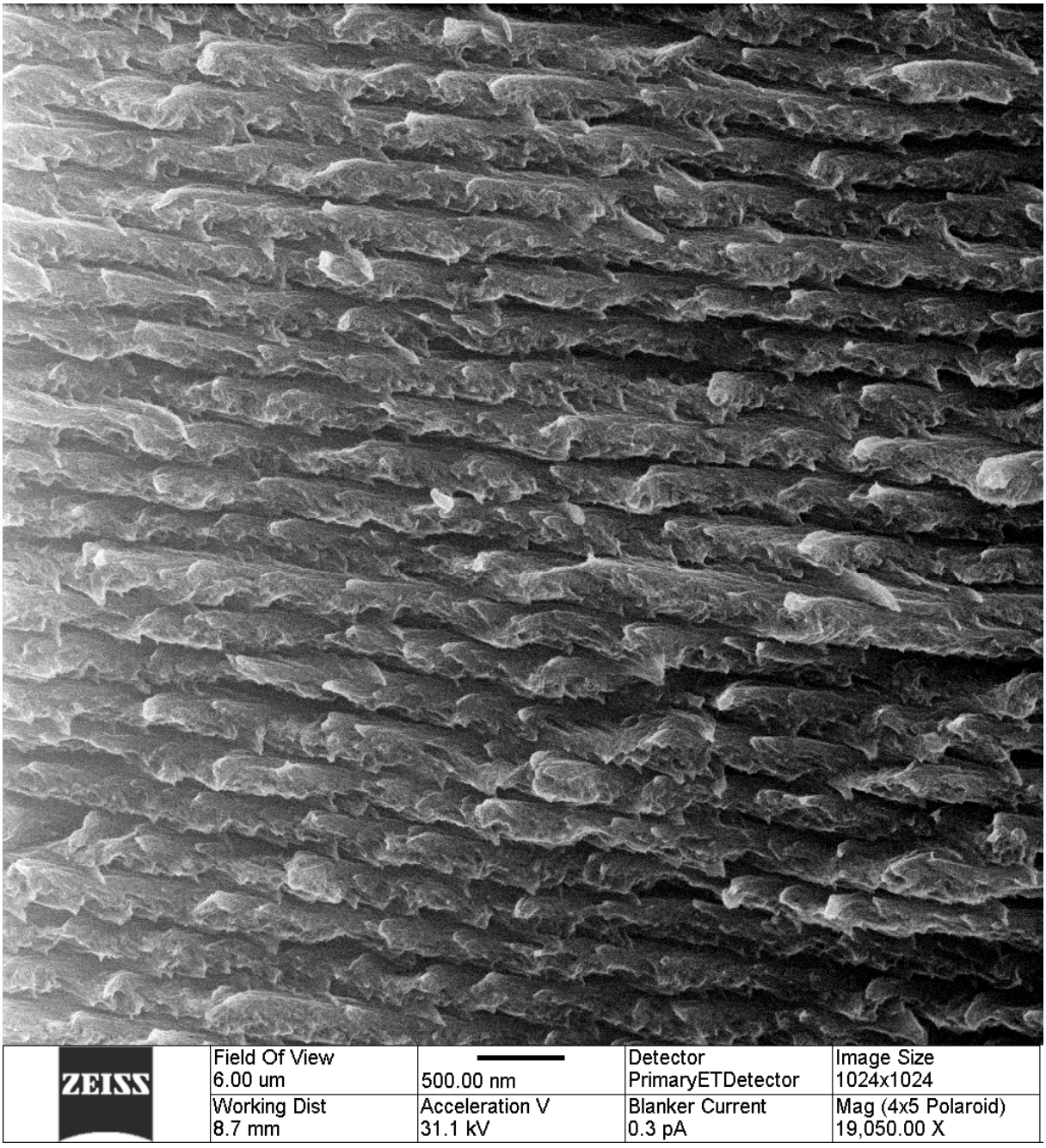

Figure S7. Expanded Figure 2c.

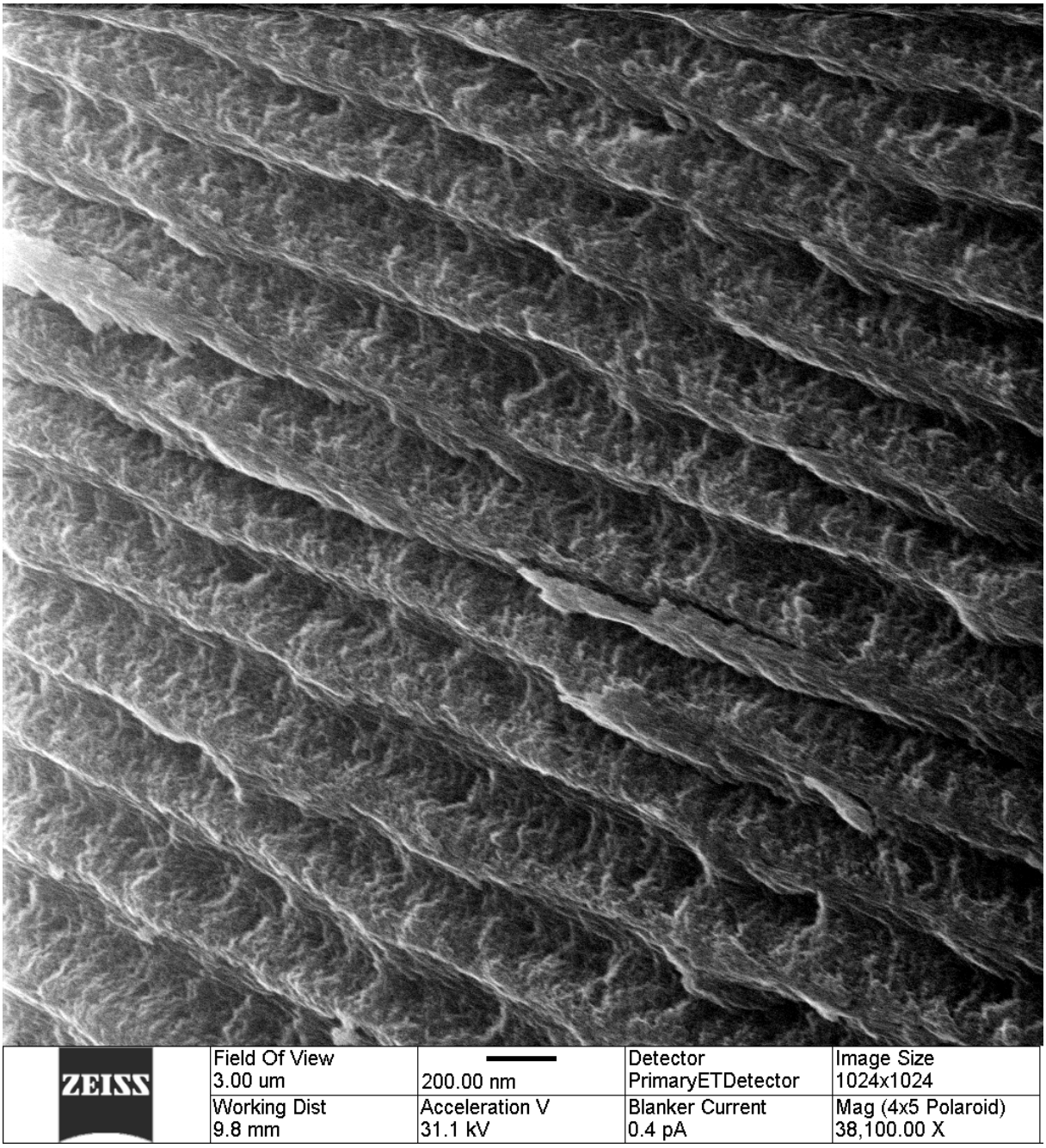

Figure S8. Expanded Figure 2d.

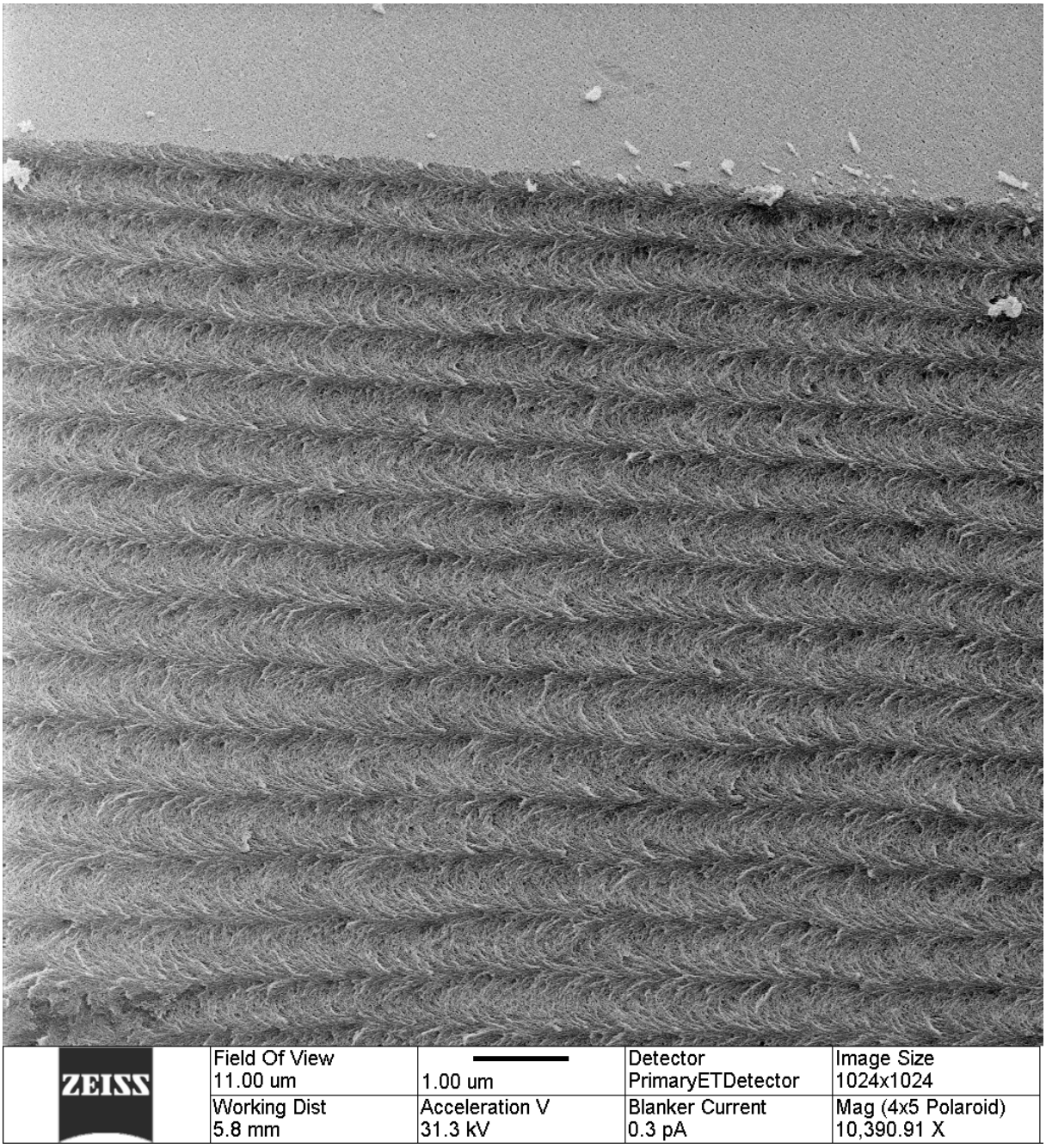

Figure S9. Expanded Figure 3a.

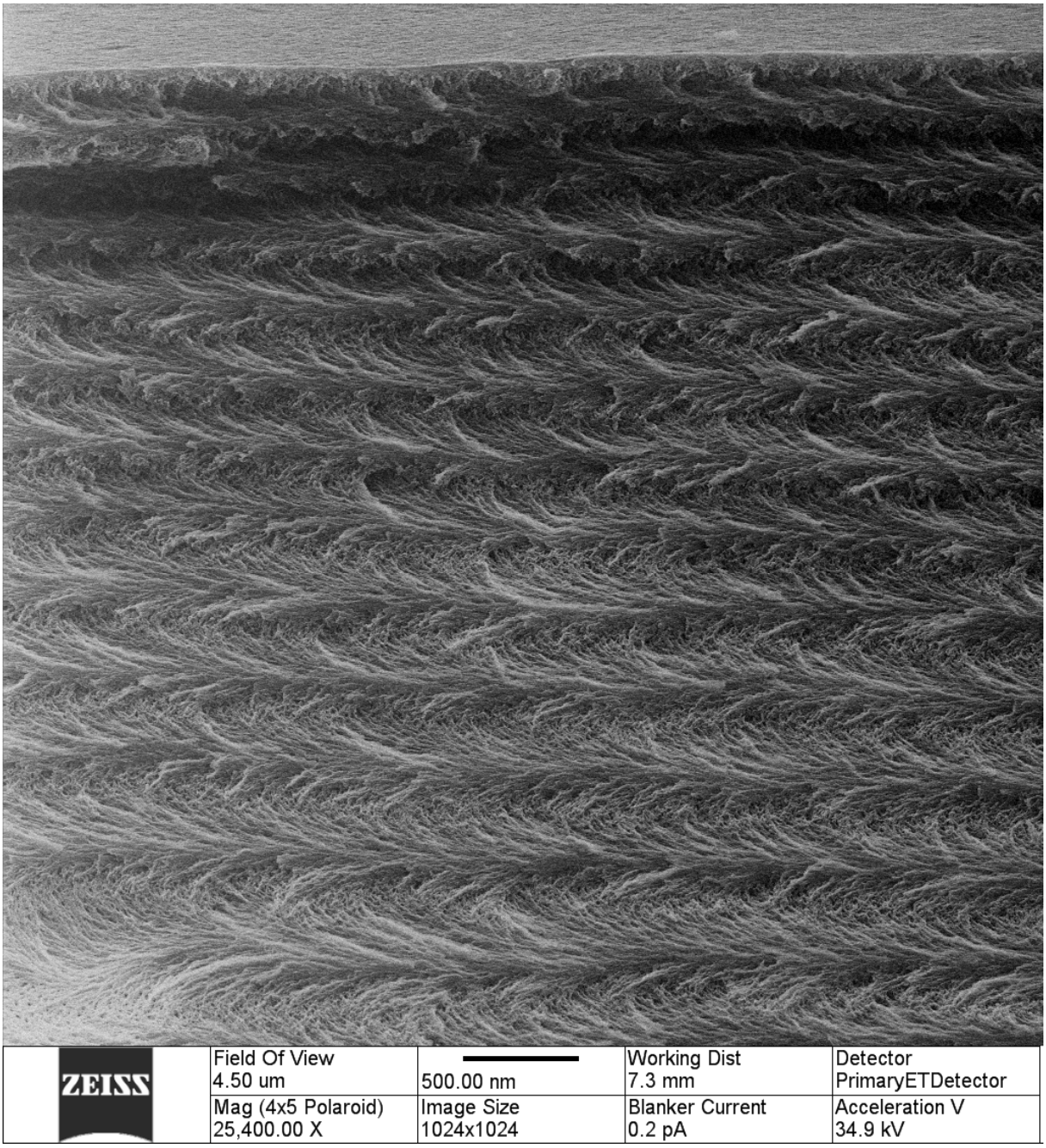

Figure S10. Expanded Figure 3b.

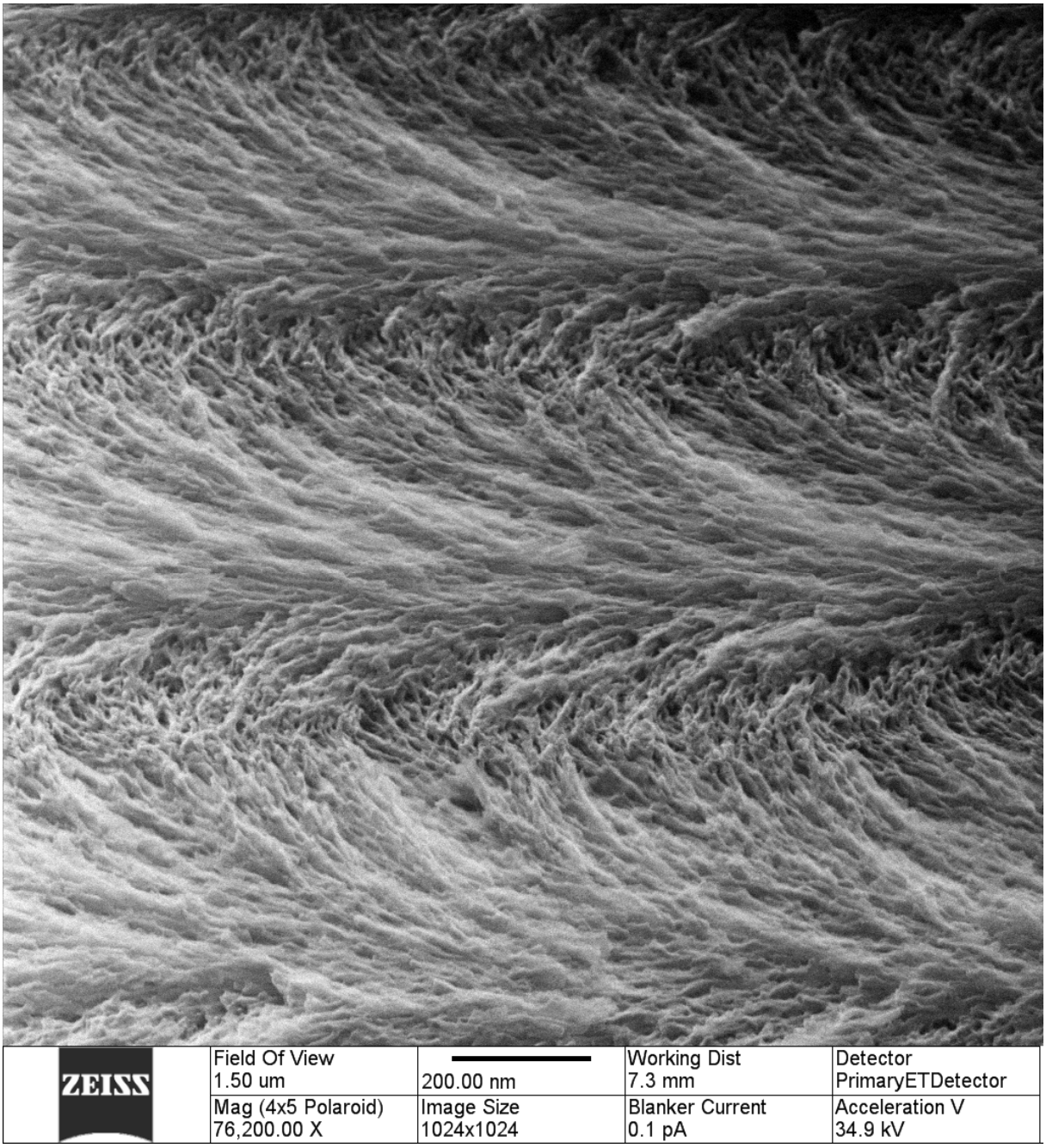

Figure S11. Expanded Figure 3c.

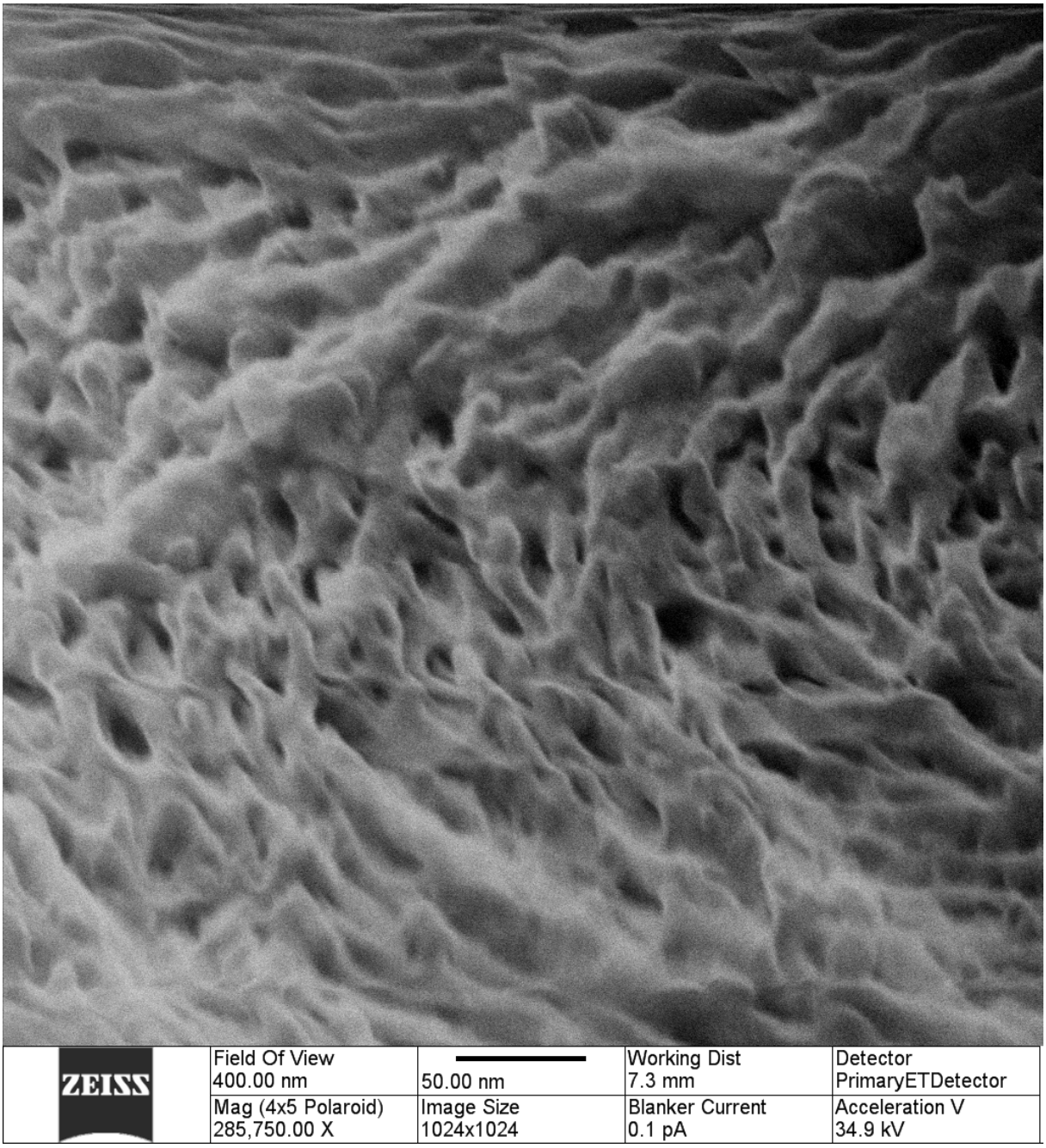

Figure S12. Expanded Figure 3d.

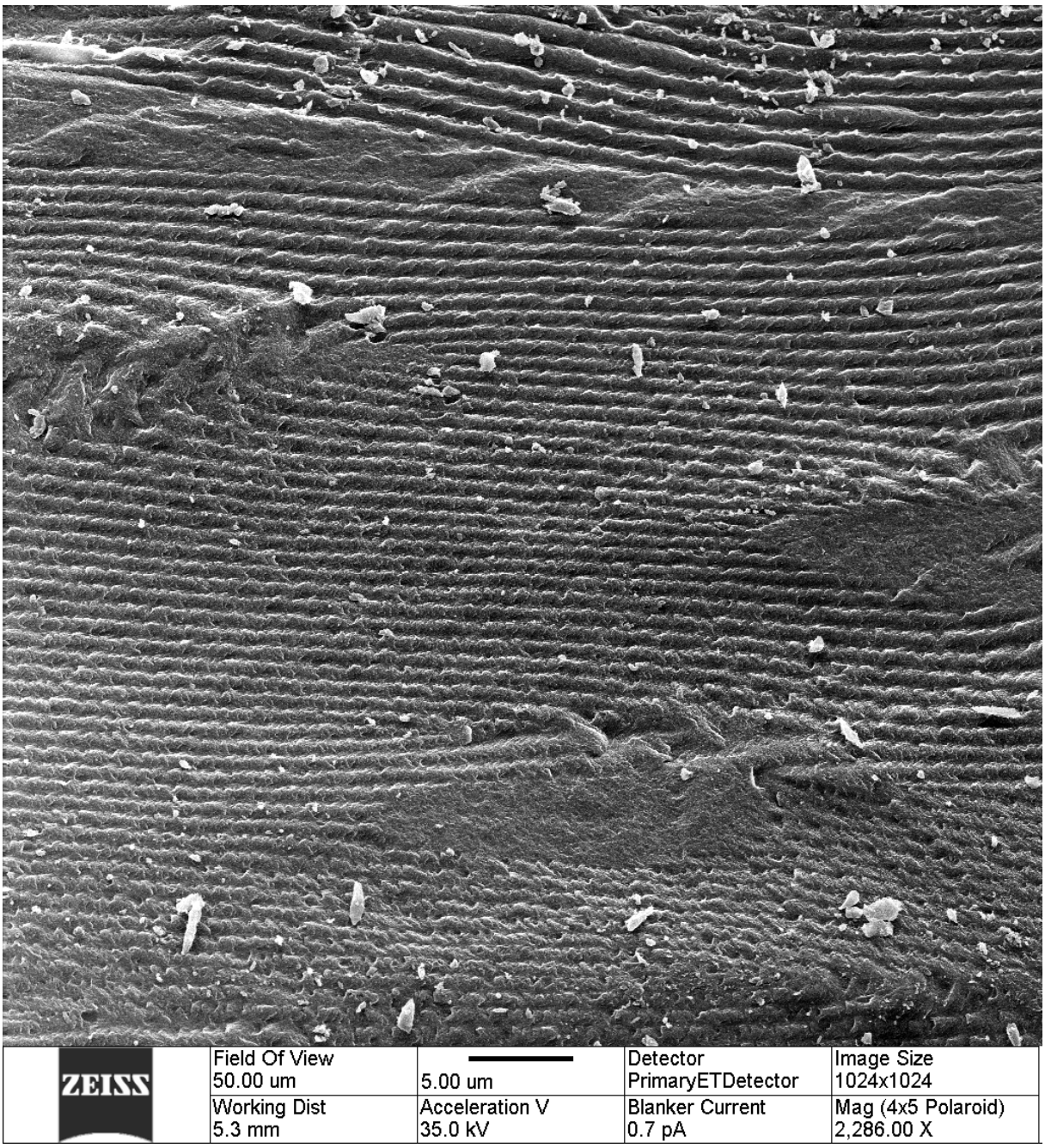

Figure S13. Expanded Figure 4a.

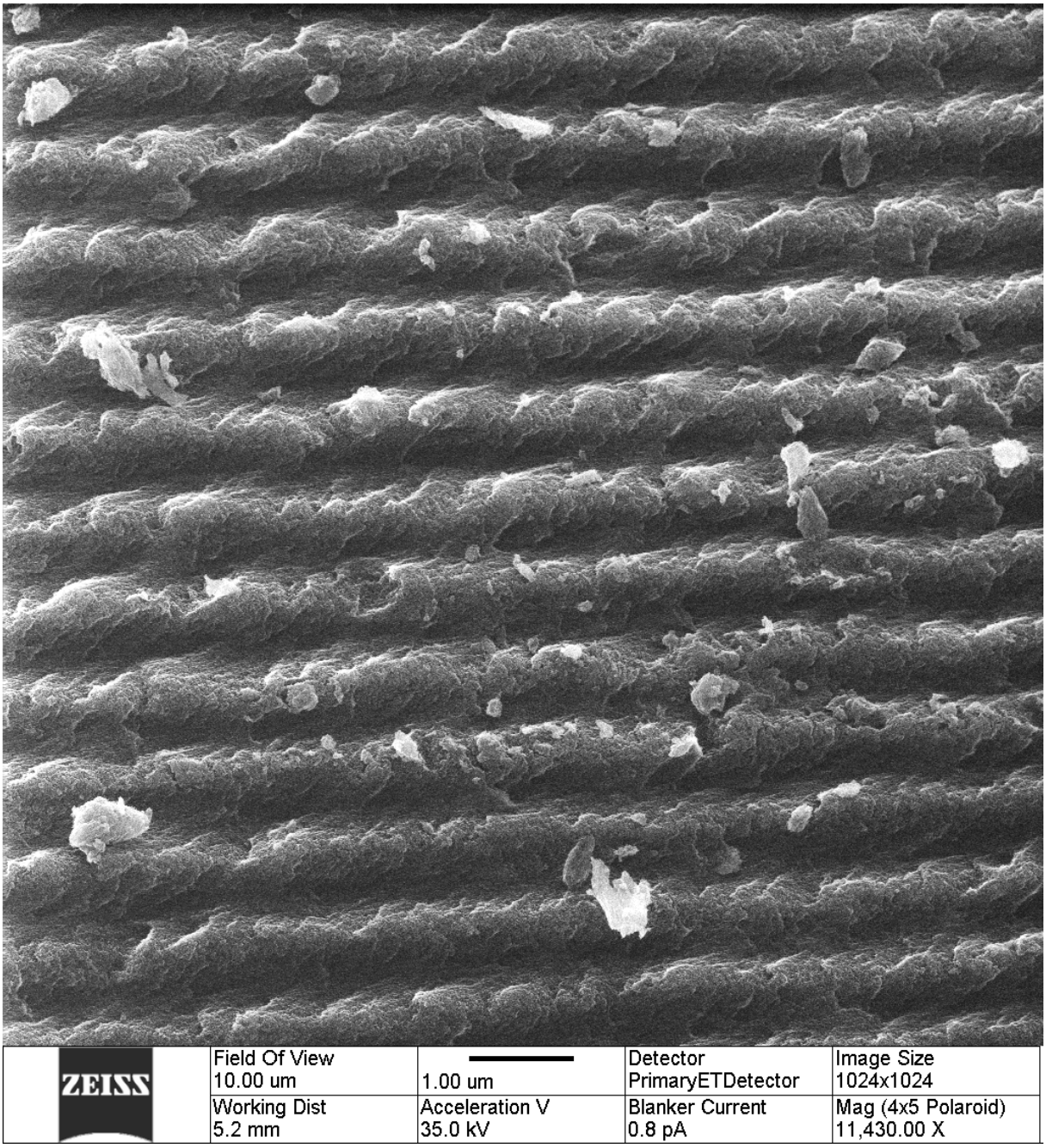

Figure S14. Expanded Figure 4b.

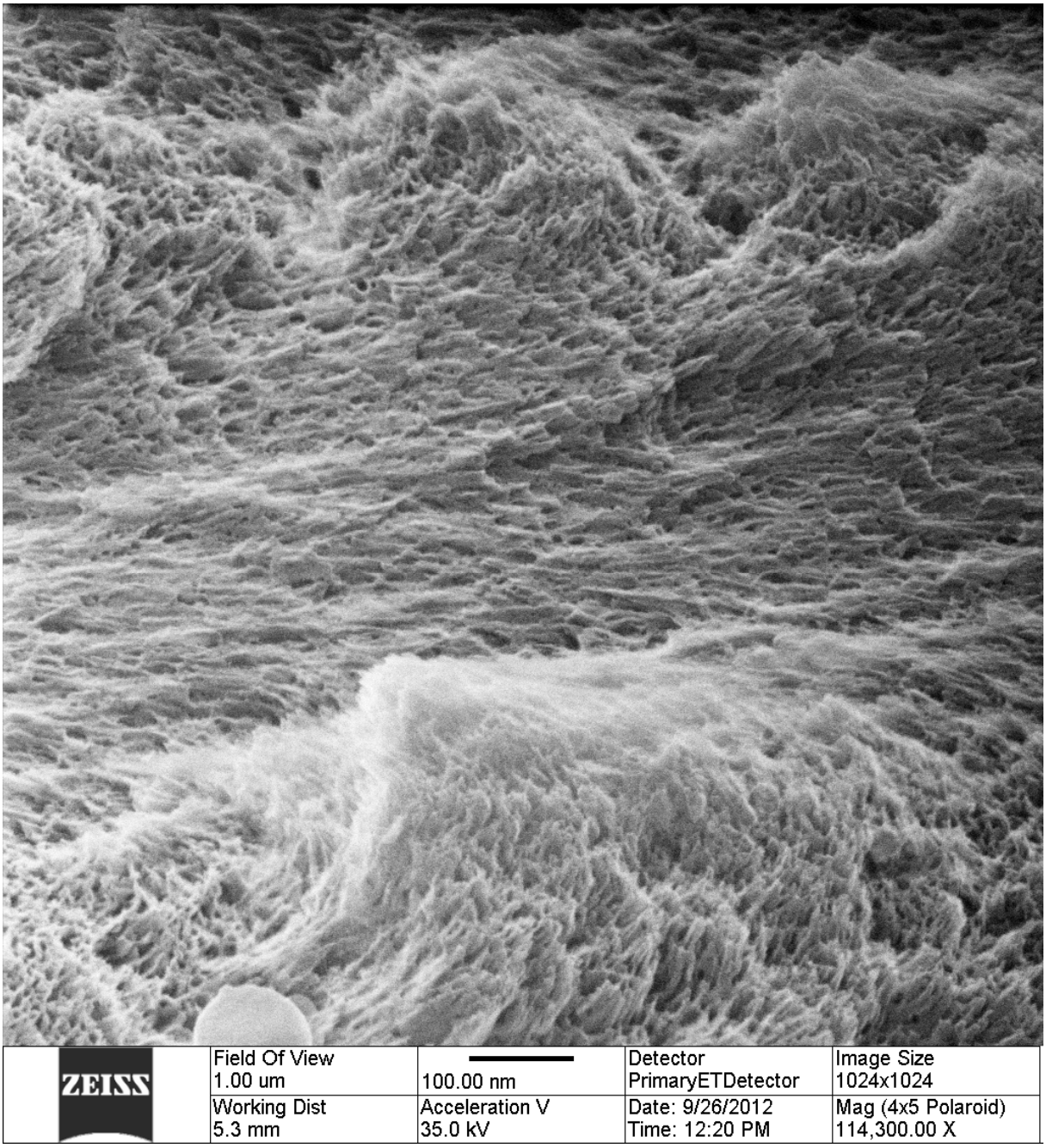

Figure S15. Expanded Figure 4c.

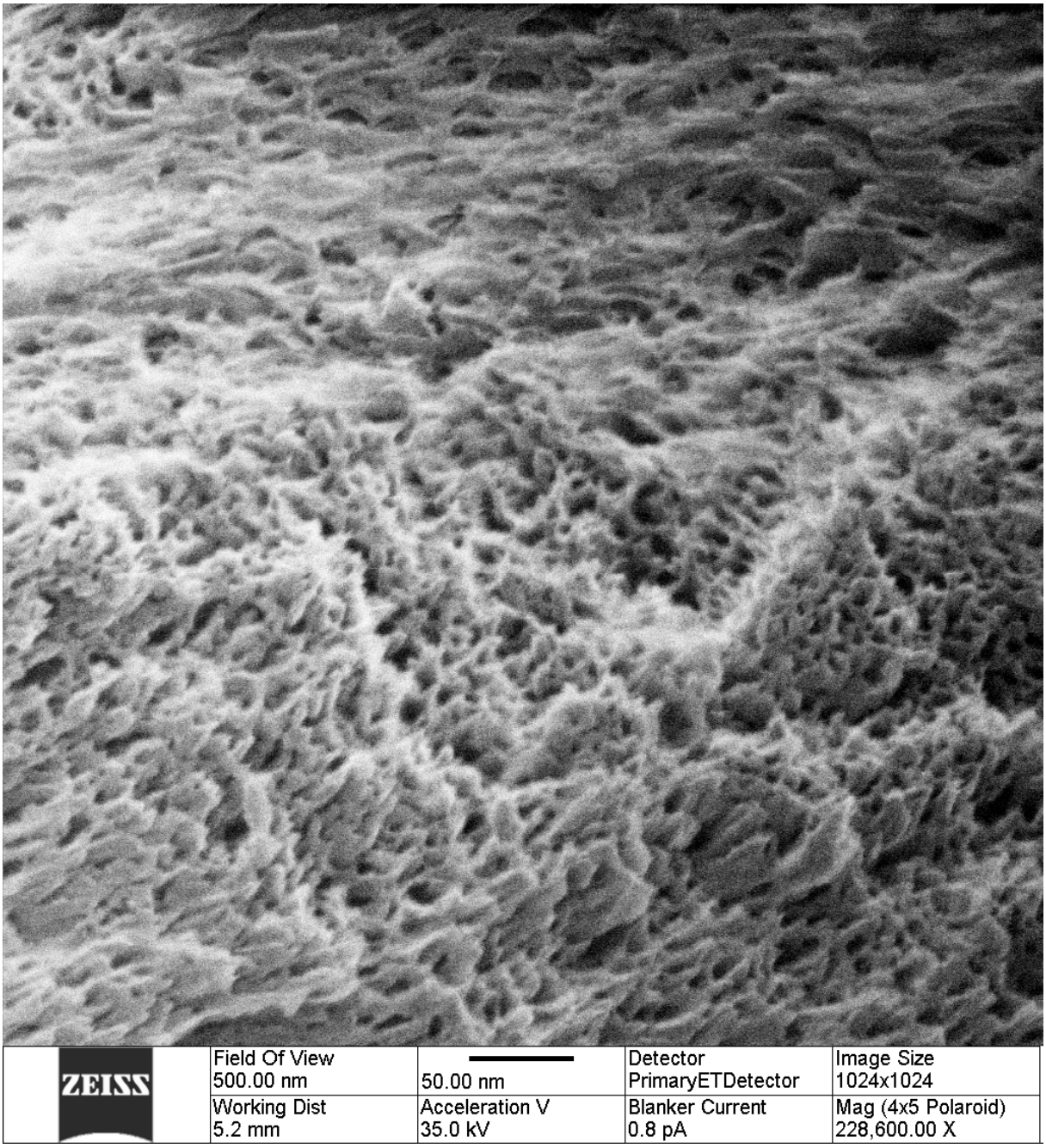

Figure S16. Expanded Figure 4d.

References

(1) K. E. Shopsowitz, H. Qi, W. Y. Hamad and M. J. MacLachlan, *Nature*, 2010**, 468**, 422.

(2) K. E. Shopsowitz, W. Y. Hamad and M. J. MacLachlan, *J. Am. Chem. Soc.*, 2012, **134**, 867.